Chapter 1
Dynamical Models of Extreme Rolling of Vessels in Head Waves

Claude Archer[1] Ed F.G. van Daalen[2] Sören Dobberschütz[3] Marie-France Godeau[1] Johan Grasman[4†] Michiel Gunsing[2] Michael Muskulus[5] Alexandr Pischanskyy[6] Marnix Wakker[6]

Abstract:
Rolling of a ship is a swinging motion around its length axis. In particular vessels transporting containers may show large amplitude roll when sailing in seas with large head waves. The dynamics of the ship is such that rolling interacts with heave being the motion of the mass point of the ship in vertical direction. Due to the shape of the hull of the vessel its heave is influenced considerably by the phase of the wave as it passes the ship. The interaction of heave and roll can be modeled by a mass-spring-pendulum system. The effect of waves is then included in the system by a periodic forcing term. In first instance the damping of the spring can be taken infinitely large making the system a pendulum with an in vertical direction periodically moving suspension. For a small angular deflection the roll motion is then described by the Mathieu equation containing a periodic forcing. If the period of the solution of the equation without forcing is about twice the period of the forcing then the oscillation gets unstable and the amplitude starts to grow. After describing this model we turn to situation that the ship is not anymore statically fixed at the fluctuating water level. It may move up and down showing a motion modeled by a damped spring. One step further we also allow for pitch, a swinging motion around a horizontal axis perpendicular to the ship. It is recommended to investigate the way waves may directly drive this mode and to determine the amount of energy that flows along this path towards the roll mode. Since at sea waves are a superposition of waves with different wavelengths, we also pay attention to the properties of such a type of forcing containing stochastic elements. It is recommended that as a measure for the occurrence of large deflections of the roll angle one should take the expected time for which a given large deflection may occur instead of the mean amplitude of the deflection.
KEYWORDS: *Mathieu equation, ship dynamics, roll, spring-pendulum systems, stochastic waves*

[1]Ecole Royale Militaire, Belgium
[2]MARIN, Wageningen, The Netherlands
[3]Universität Bremen, Germany
[4]Wageningen University and Research Centre, The Netherlands
[5]Leiden University, The Netherlands
[6]Delft University of Technology, The Netherlands
[†]corresponding author: `johan.grasman@wur.nl`

1.1 Introduction

On October 20th, 1998, a post-Panamax C11 class cargo ship sailed on the Pacific from Taiwan to Seattle. While traversing a heavy storm, the vessel began an extreme rolling motion (transversal swinging) with an angle of up to 40 degrees to each side. After the storm had settled, the crew examined the status of the cargo and found that one third of the containers were lost and another third heavily damaged, making this incident the greatest container casualty known so far (cf. France et al. [9] for a detailed account of the events).

The ship experienced a phenomenon known as "parametric roll" or "parametric resonance": During only a few roll cycles, the roll angle increases far above what would be considered normal (mostly up to 10 degrees). This behaviour of a ship had been known from the 1950s, but only considered to be relevant for smaller vessels in following seas (cf. [26]).

After the October 1998 incident, interest has been renewed. It has been suggested by Shin et al. [26] that the hull shape of modern container ships might increase the risk of parametric roll. In order to enlarge the load capacity while keeping the water resistance small, the length and width of ships increased and a wide, flat stern and pronounced bow flares appeared. This had an effect on the ship's stability when encountering waves.

Possible countermeasures to avoid heavy rolling include the attachment of stabilizing fins to the outer hull of the ship or the installation of active water tanks in the interior of the ship. However, these actions increase the fuel consumption and lessen the number of containers which can be carried. That is why these techniques are not used for modern cargo ships (cf. [26]).

Obviously, the estimation of the risk of parametric resonance for a given ship geometry and load characteristic is of great importance to ship owners and constructors. Research centres such as the Marine Research Institute Netherlands (MARIN) therefore try to predict the probability of the occurrence of parametric roll by using computer simulations and model tests.

This paper reviews models for describing the excitation of the rolling motion. Methods for analyzing autoparametric resonance in mechanical systems ([30]) are applied to three different models: the variable length pendulum model (Section 1.2), the spring-pendulum model (Section 1.3) and the spring-double pendulum model, see Section 1.4. These models describe a ship as a force-driven dynamical system of springs and pendulums with one up to three degrees of freedom. However, these models only consider a single encounter frequency. To account for the more realistic situation of a superposition of different waves we add up different waves containing stochastic elements in a way that an appropriate

type of spectrum is composed, see Section 1.5.

1.1.1 Shape of a vessel and its metacentric height

In this part, we discuss the main causes of this sudden large amplitude rolling motion [26], such as the new design of the hull of container ships influencing the stability under heavy weather conditions and the phenomenon of parametric resonance as it applies to roll dynamics.

In the seventies, ships had a payload of about 2000 containers and were able to sail at about 25 knots. Nowadays, some container ships are built to carry 10000 containers, or even more, and are still sailing at the same speed. To achieve this without increasing the fuel consumption, it was necessary to give thinner shapes to hulls. Consequently:

- Ships are longer and their length now approximately corresponds to the length of waves as they are met in the Pacific and the North Atlantic Ocean.
- The bow and stern shapes are thinner and more extended to the centre of the ship, the section in the centre with a fixed U-shaped cross-section of the hull is now forming a much smaller proportion of the ship, see Figure 1.1.

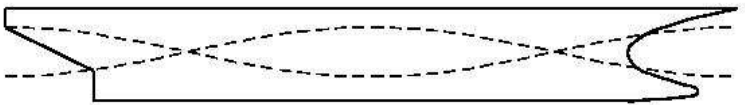

Figure 1.1: Change in waterline surface of a ship at different phases of the passing wave.

These two aspects have as consequence that, when the ship encounters waves, its changed dynamical characteristics may bring about a critical response (Figure 1.2). Most important factor is the varying metacentric height of the ship, this is a vector pointing to the centre of gravity of the vessel with the centre of buoyancy as origin (the centre of buoyancy is the gravity centre of the displaced body of water). The averaged transverse cross-section of the vessel yields the transverse component (GM) of the metacentric height, see Figure 1.2. This component determines for a large part the roll amplitude. If the ship length is about the length of the incoming wave, the ship periodically passes two extremes with the middle of the ship at a crest or in a trough. From Figure 1.1 it is seen that this makes for a large difference in buoyancy. Consequently, the restoring force

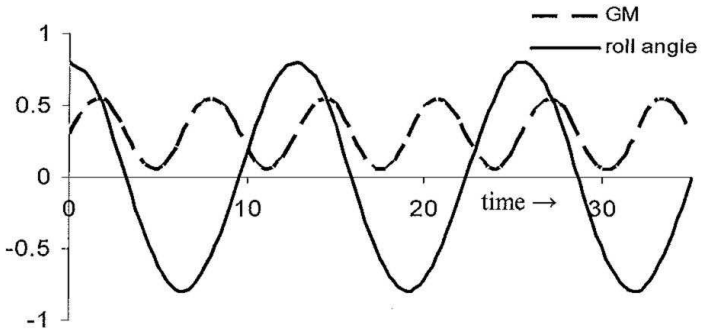

Figure 1.2: Roll angle in the course of time in the resonant state. Note that the period is twice the period of the wave. The dotted line denotes the variation of the metracentric height GM from the waves.

varies a lot. The GM represents indirectly the righting lever $GZ = GMsin\phi$, where ϕ is the roll angle, see Figure 1.3.

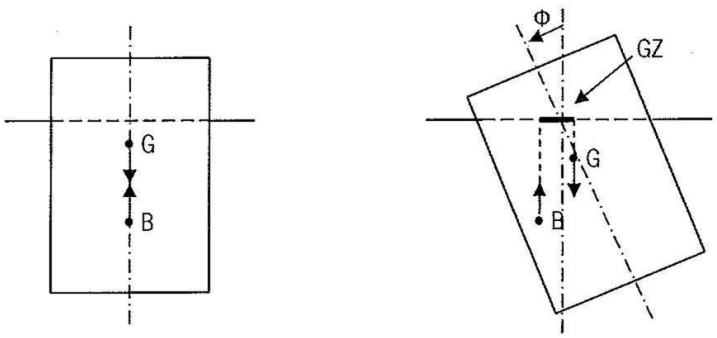

Figure 1.3: Cross section of a floating container. The line that connects the centre of buoyancy B with the gravity centre G of the container represents the metacentric height. (a) The rest state; note that the gravity force is compensated by the upward force of the displaced body of water. (b) The container is out of balance; the centre of buoyancy has moved to the left. The two forces are balanced in the vertical direction, but cause a (clockwise) restoring moment GZ equal to the projection of the metacentric height GM (line BG) upon the horizontal axis.

When the ship is on the crest of a head wave whose length is about the length of the ship, the waterline surface of the ship (surface area defined by the intersection of the hull and the water surface) takes a minimum value. Correspondingly GZ as well as the roll stability are both at a minimum. Vice versa, GM and the stability are at their maximum when the ship is in the trough of the wave. These successive variations of stability can cause large roll motions. Since this phenomenon occurs with waves affecting the restoring

force with a frequency being about twice the natural roll frequency and results in a large roll amplitude, it is called parametric resonance. In Figure 1.3 the different stages of the roll cycle can be discerned. When the ship is away from the vertical (0 degrees angle) and in a deep trough, the righting lever is larger than in calm water, and the ship comes back faster to the vertical while accumulating kinetic energy. At the end of the first quarter of the roll period, the ship crosses the vertical and continues its move to the other side because of the inertia. During this second quarter of the roll period, the ship is on a crest, so the righting lever is smaller than in calm water, and the ship continues its movement to a larger roll angle, due to the accumulated kinetic energy. In the third quarter the action of the first quarter is repeated at the opposite side and the fourth quarter mirrors the second quarter.

1.1.2 Extreme rolling

The rolling motion may re-enforce itself so that the amplitude of the roll motion increases within a couple of roll periods from a few degrees to about 40 degrees. The resonant dynamics from a periodic change of the GM due to waves coming in with a frequency being twice the natural frequency is best understood from a pendulum whose length varies with time. The amplitude of such a pendulum can be increased if its length varied in such a way that it is smaller when it moves away from the vertical and larger when it gets close to the vertical. This means that the length must vary with a frequency that is twice the natural frequency of the pendulum. The GM of the ship can be seen as the length of the pendulum. This phenomenon is similar to a child sitting on a swing who tries to get higher by being seated when the swing gets close to the vertical and getting up when it moves away from the vertical. The centre of gravity of the child then rises (smaller pendulum length) and falls (larger pendulum length) successively making the swing a (parametricly) resonant system which we will discuss in Section 1.2.

For getting parametric roll in case of a rolling vessel, some conditions must be fulfilled:

- The length of an incoming wave is about the length of the ship
- The waterline surface of the ship varies considerably during a wave cycle
- The encounter frequency of the waves is about twice the natural roll frequency of the ship

1.1.3 Models with more than one degree of freedom (DOF)

In spite of these apparently strict conditions, it's still very difficult to accurately estimate the risk of occurrence of parametric roll. It is our aim to select mathematical models that suitably can be used for numerical simulations based on naval architecture data. Eissa et al. [6] describe a 2-DOF nonlinear spring pendulum model. By multiple time scale perturbation techniques, approximations of the solutions up to 4th order are obtained, together with stability regions and solvability conditions.

A 3-DOF nonlinear model was developed by Neves [23], Neves and Rodriguez [24], using a Taylor-series expansion up to second (and later to third) order of the damping and restoring forces. The governing equations are found to be a coupled system of Hill equations ([12]), with the parameters given explicitly by the ship's characteristics and geometry. This model has been implemented in MATLAB by Holden et al. [13] and is now a part of the Marine Systems Simulator[1].

1.2 The Parametric Pendulum (1-DOF)

The swing analogy leads to the differential equation of a variable length pendulum. The general 1-DOF equation for the roll angle ϕ is

$$(I + A)\frac{d^2\phi}{dt^2} + B\frac{d\phi}{dt} + C(t)sin(\phi) = 0, \tag{1.1}$$

where $C(t)$ is the restoring force, I the ship inertia, A the added mass and B the damping in the roll direction ([17], [10]). The restoring force is $GZ = GMsin(\phi)$. For small angle it is linearised as $GZ = GM\phi$. Dunwoody [5] showed that in calm water GM oscillates around its mean value GM_m and also that the amplitude GM_a of the oscillation is proportional to the wave elevation. In the case of a single frequency wave with angular velocity ω, Dunwoody's results give

$$C(t) = \rho g\Delta(GM_m + GM_a cos(\omega t)), \tag{1.2}$$

where Δ is the displacement of the ship (water equivalent of the immersed volume of the ship), ρ the water density and g the gravity constant. If the pendulum angle ϕ is small Eq.(1.1) can be linearized taking the form of the periodically forced Mathieu equation, see Tondl [30]:

$$\frac{d^2\phi}{dt^2} + b\frac{d\phi}{dt} + (c + dcos(\omega t))\phi = 0, \tag{1.3}$$

[1] Available under a GNU General Public License, see www.marinecontrol.org.

where b is the damping coefficient, c the coefficient of the restoring force and d and ω respectively the amplitude and angular velocity or frequency of the periodic forcing. The natural frequency ($d = 0$) is

$$\omega_0 = \sqrt{c - b^2/4}. \tag{1.4}$$

for which resonance behavior for a forcing at twice the natural frequency is well known. More general the phenomenon may occur for any periodic forcing term. The corresponding differential equation is then referred to in the literature as a Hill equation, see Hochstadt [12].

1.2.1 A threshold for parametric roll

In [10] the threshold for parametric roll has been studied for both the original and the linearized restoring force term. We have seen before that the restoring force of the ship against rolling is larger when the wave trough is amidships than when a wave crest arrives at this point. This is due to the variation of GM. Let δGM be the difference of GM between these two extreme cases and let $p = \delta GM/GM_m$ be the proportion that represents this variation with respect to the calm water GM_m. A large ratio p corresponds to a high probability of having parametric roll. The threshold for parametric roll is then expressed as the critical minimal value of p for which a large response (resonance) occurs. For the Mathieu equation ([30]) this critical value can be estimated for a given ω. For a ship model it has been predicted in [10] that parametric roll starts when $p > 4\mu/\omega_0$ with damping ratio $\mu = \frac{1}{2}B\omega_0/((I + A)\omega_0)$ and ω_0 given by (1.4). An accurate determination of the damping ratio μ is crucial as it will strongly influence the model prediction.

In [17], this threshold has been validated against basin data for a simple hull form and compared with results from the full non-linear time domain seakeeping code PRETTI developed for improving the computation of the effect of hull forms (not yet tested in a basin). The authors conclude that the 1-DOF model can very well be employed in preliminary hull design with a damping factor μ tuned with the use of empirical data. It gives an idea of the threshold wave height for which parametric roll occurs. For the estimation of the amplitude of the actual roll angle a nonlinear model is needed for which for example the code PRETTI can be used. Of course this requires more computing time.

1.2.2 Further investigations

Most of the literature on parametric roll focusses on two approaches: the derivation and theoretical analysis of a mathematical point-ship model and/or the numerical implementation of such a model using the appropriate vessel and wave specifications.

France et al. [9] and Shin et al. [26] considered a 1 degree-of-freedom (DOF) ship model. By linearizing the moments of damping and restoring, the authors arrive at a Mathieu-equation to describe the ship's behaviour. However, Spyrou [28] pointed out several disadvantages of linearized models: the linearization is only valid for small roll angles, whereas parametric roll is characterised by large roll amplitudes. In addition, the instability regions of Mathieu-type models reflect the behaviour given an infinite number of roll cycles – but we already mentioned that parametric roll only takes a few of them to build up.

1.3 A Model for Heave-Roll Motion(2-DOF's)

The specification of resonance conditions is one of the most important topics in the prediction of parametric roll. Running large scale models formulated by researchers and engineers may need hours or even days of computing time so that a quick estimate of parameters relevant for roll cannot be obtained from it. Therefore, research is also directed to the formulation of low dimensional models or simple schemes which may predict heavy rolling given certain operational conditions. In this section one of such models will be considered, see Figure 4.

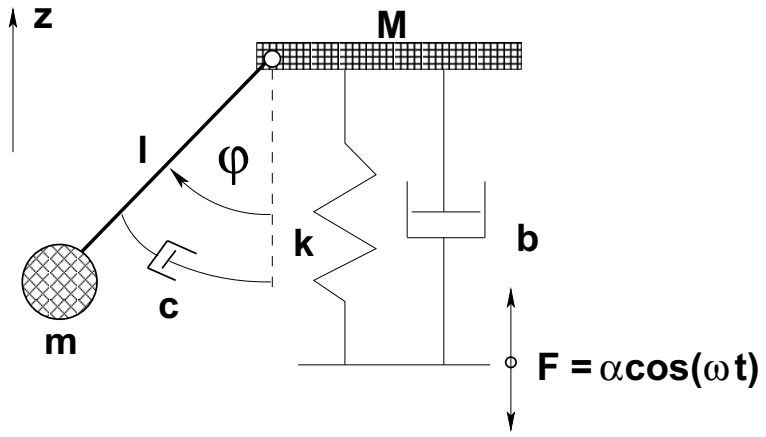

Figure 1.4: Driven spring-pendulum model for heave-roll motion.

It is a two degrees of freedom model formulated by Tondl et al. [30] consisting of a mass mounted to a periodically moving floor by a linearly damped spring. In addition a pendulum is connected to this mass. An external periodic force of the form $\alpha\cos(\omega t)$ is applied to the floor with α and ω respectively amplitude and frequency of the external

periodic force. This system satisfies the following two coupled differential equations:

$$\begin{aligned}&(M+m)(\ddot{z}-\alpha\omega^2 cos(\omega t))+b\dot{z}+kz+ml(\ddot{\phi}sin(\phi)+\dot{\phi}^2 cos(\phi))=0,\\&ml^2\ddot{\phi}+c\dot{\phi}+mglsin(\phi)+ml(\ddot{z}-\alpha\omega^2 cos(\omega t))sin(\phi)=0.\end{aligned} \tag{1.5}$$

After carrying out transformations of the time- and the dependent variables and making a small perturbation approximation the system is described by the following dimensionless linear differential equations:

$$\begin{aligned}&\ddot{u}+\kappa\dot{u}+q^2u=0,\\&\ddot{\psi}+\kappa_0\dot{\psi}+\psi-a\eta^2\left[(1+A)\cos(\eta\tau)+B\sin(\eta\tau)\right]\psi=0,\end{aligned} \tag{1.6}$$

where u and ψ are the vertical and the angular displacements of respectively the mass and the pendulum, $\kappa_0 = c/(\omega_0 ml^2)$, $a = \alpha/l$, $\eta = \omega/\omega_0$ and

$$A = \frac{\eta^2(q^2-\eta^2)}{\Delta},\ B = \frac{\kappa\eta^3}{\Delta},$$

with $\Delta = (q^2-\eta^2)^2+(\kappa\eta)^2$, $q^2 = k/(\omega_0^2(M+m))$, $\kappa = b/(\omega_0(M+m))$. Here m is the mass of the pendulum, M is the mass of the oscillator, l is the length of the pendulums weightless rod, ω_0 is the eigenfrequency of the oscillator, b and c are the damping coefficients of the linear and angular motions, k is the stiffness coefficient of the spring, and the dot denotes the derivative with respect to the time variable τ.

The value of the parameter η determines for a large part the stability of the rolling motion. For a value close to 2 an unstable motion may occur with large angular deflections of the pendulum. This only happens if the forcing amplitude a is above a threshold. In [30] it is derived that this threshold depends on η and the other parameters in the following way:

$$a_{lin} = \frac{2}{\eta^2}\left[\frac{\left(1-\frac{1}{4}\eta^2\right)^2+\frac{1}{4}\kappa_0^2\eta^2}{(1+A)^2+B^2}\right]^{1/2}, \tag{1.7}$$

Thus, for a ship-wave system Eq.(1.7) represents the value of the amplitude of regular wave with a fixed frequency above which the equilibrium gets unstable. For a vessel it means that heavy rolling may build up in a short time.

1.3.1 Computation of the threshold values from experimental data

This section deals with four experiments with physical models in the form of scaled ships towed in a basin. In addition at MARIN computations are carried out for these ships

using a potential flow code (PFC). For each case these numerical investigations yield estimates for parameters occurring in Eq.(1.7). Two of the MARIN experiments are related to a vessel X with two different input data-sets. Parametric rolling has been observed during the experiments and was confirmed by the model computations. The third experiment with vessel Y did not show parametric roll which is in agreement with the computations using PFC. In the last experiment related to the vessel Z parametric roll was observed during the tests of the physical scaled model in the basin. However, in this case it was not predicted by the computations. All experiments were carried out with head waves acting upon the vessel.

The input data-sets for the models include the following parameters: the frequency of the external force ω [rad/s], the heave and the roll damping coefficients being respectively b and c and the stiffness coefficient k. The data-sets have been computed by MARIN using PFC for a range of frequencies of the excitation force, and were given to us to analyse them using the results of the linear approximation Eq.(1.6). It is noted that the threshold amplitude Eq.(1.7) does not explicitly depend on the speed of the waves (or the vessel). Of course, the speed is implicitly present in the input data (Doppler effect).

Substituting the input data into Eq.(1.7) the threshold amplitude a_{lin} we obtain for each of the four vessels. However, some transformations and additional calculations have to be made first. The length l of the pendulum can be found using the well-known equation of the period of small oscillations of the physical pendulum $T = 2\pi\sqrt{l/g}$, where T is the roll period of the ship, l is the length of the 'equivalent' mathematical pendulum satisfying $l = gT^2/(4\pi^2)$. Since the rolling does not depend directly on the wave excitation but on the heave motion of the vessel, a transfer function is needed. Thus the final threshold amplitude for the waves can be written as

$$a_{thr} = \frac{a_{lin} l \omega^2 M_h}{S(\omega)}, \tag{1.8}$$

where M_h is the mass of the vessel moved by the heave motion and $S(\omega)$ the transfer function taken from the 'MARIN' data.

To simplify the calculations a C-code program has been written in such a way that the threshold amplitude a_{thr} directly can be obtained from the input data-set for each value of the frequency of the excitation force. The graphs of the threshold amplitude for each set of data (for each vessel) are presented in Figure 1.5.

Parametric resonance of the vessel for all models can most likely be expected in the range of small frequencies of the external force up to 0.8 [rad/s], with values for the amplitude of the waves from around 0.4 to around 30 meters. These threshold amplitudes

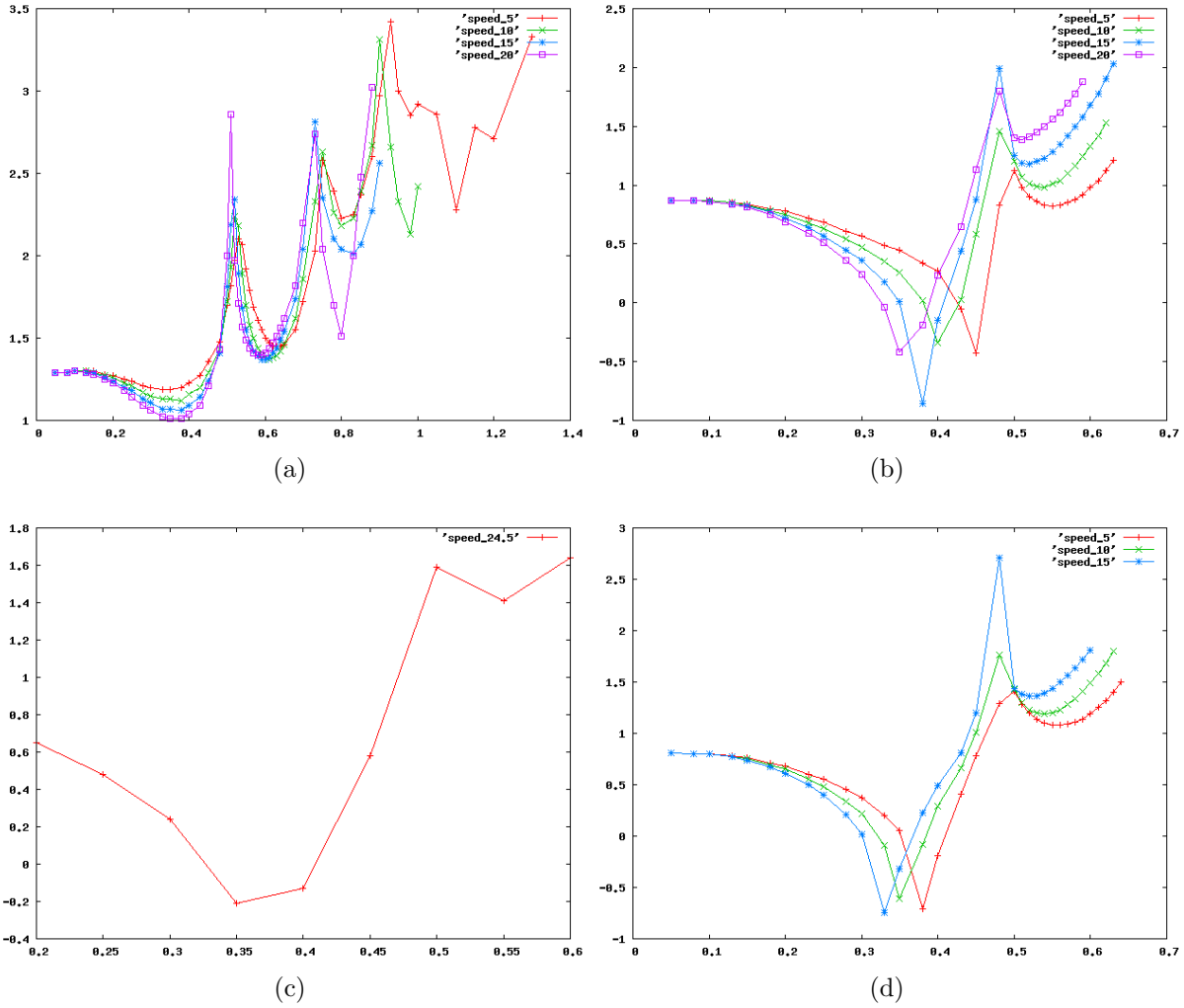

Figure 1.5: Logarithm of threshold amplitudes α of a single frequency wave forcing as a function of the wave frequency ω for different speeds of the vessel. (a) Vessel X for a large range of wave frequencies. (b) Vessel X for low frequency waves in more detail; note the low threshold value at $\omega = 0.4$. (c) For vessel Y a similar, but less pronounced, resonance is found. (d) Result for vessel Z.

can be so small because all energy goes in that wave with a single frequency. In reality waves consisting of various stochastic components will increase these values considerably. The parts of the graphs for the higher frequencies are cut out because the values of the threshold amplitude are very large.

1.4 A Spring with Two Pendulums (3-DOF's)

For further study of ships, we define our coordinate vectors as $\vec{x}$ pointing from the center of mass towards the front of the ship while $\vec{y}$ and $\vec{z}$ are pointing towards the right side of the ship and in the upwards vertical direction, respectively. We know that roll and pitch (rotation around resp. the x and the y axis) and heave (movement in the z direction) are strongly coupled. The important question is now: under what conditions is it possible that pitch and heave motion are rapidly converted into roll motion? As a first observation we should mention that the moment of inertia for pitch is much larger than the one for roll. This means that even for small pitch angles a potentially dangerous amount of angular momentum is stored in pitch.

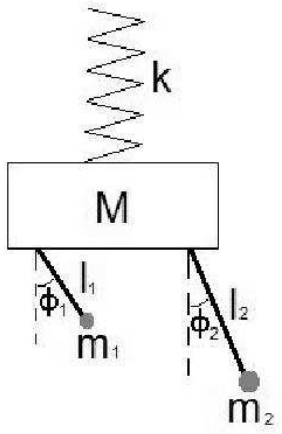

Figure 1.6: Spring and two-pendulum model for heave-roll-pitch motion. Note that in this model there is no direct interaction between roll and pitch.

In a spring - pendulum model (SPM) the pendulum accounts for roll and the spring accounts for heave, see Tondl et al.[30]. In this publication also the double spring - pendulum model (DSPM) is introduced, so that also pitch is included. The system consists of two springs connected by a rod that turns freely around its length axis. A pendulum, connected to this rod, models the roll of the ship, while the two springs capture

heave and pitch. Because in this model heave and pitch are identified by separate state variables, it is not possible to see the effect of "pitch energy" being released. Instead of the DSPM, we prefer to present the spring - double pendulum model (SDPM), see Figure 1.4. It consists of a large mass M (related to the mass of the ship) mounted by a vertical spring to a fixed point. The spring constant k represents the restoring force component in the heave mode. The position of the fixed point may change in time denoting forcing by waves. The pendulums have masses m_i attached to the large mass by rods of length l_i, see Figure . It is assumed that the pendulums swing independent from each other (physically in directions perpendicular to each other) and that they only interact via the heave motion. The product $m_1(l_1)^2$ is determined by the moment of inertia around the x axis (roll), $m_2(l_2)^2$ is determined by the moment of inertia around the y axis (pitch). The three degrees of freedom of this system are z, ϕ_1 and ϕ_2 being the vertical displacement of mass M from the stationary state and the angles with the vertical for both pendulums. The kinetic energy is given by

$$T = \frac{1}{2}M\dot{z}^2 + \sum_{i=1}^{2}\left[\frac{1}{2}m_i\left(\dot{z} + l_i\dot{\phi}_i\sin\phi_i\right)^2 + \frac{1}{2}m_i\left(l_i\dot{\phi}_i\cos\phi_i\right)^2\right], \tag{1.9}$$

and the potential energy is given by

$$V = \frac{1}{2}kz^2 + \sum_{i=1}^{2} m_i g l_i(1-\cos\phi_i). \tag{1.10}$$

Since the heavy sideway roll in practice appears within a few periods, we assume that external forcing cannot account for this effect. Therefore we do not include an external force. Of course the initial heave and pitch are caused by an external pulse or by setting a far from equilibrium initial state. We investigate the conditions for transfer of heave and pitch into roll.

1.4.1 Equations of Motion

For the Lagrangian $L = T - V$, the Euler-Lagrange equation for variable u is given by

$$\frac{d}{dt}\frac{\partial L}{\partial \dot{u}} - \frac{\partial L}{\partial u} = 0. \tag{1.11}$$

For the model under consideration, the Lagrange equations are found to be

$$\begin{aligned}(M+m_1+m_2)\ddot{z} + b\dot{z} + kz + m_1 l_1(\ddot{\phi}_1\sin\phi_1 + \dot{\phi}_1^2\cos\phi_1)\\ +m_2 l_2(\ddot{\phi}_2\sin\phi_2 + \dot{\phi}_2^2\cos\phi_2) = 0,\end{aligned} \tag{1.12a}$$

$$l_1\ddot{\phi}_1 + c_1\dot{\phi}_1 + g\sin\phi_1 + \ddot{z}\sin\phi_1 = 0, \tag{1.12b}$$

$$l_2\ddot{\phi}_2 + c_2\dot{\phi}_2 + g\sin\phi_2 + \ddot{z}\sin\phi_2 = 0, \tag{1.12c}$$

where b, c_1, and c_2 are the damping coefficients and g is the gravitation acceleration. A large amplitude response from a periodic forcing is expected if the damping terms are small. Therefore, in our model we neglect these terms. Eqs. (1.12) are linearized using the small angle approximation:

$$\begin{aligned}(M + m_1 + m_2)\ddot{z} + kz + m_1 l_1(\ddot{\phi}_1\phi_1 + \dot{\phi}_1^2 - \frac{1}{2}\dot{\phi}_1^2\phi_1^2) \\ + m_2 l_2(\ddot{\phi}_2\phi_2 + \dot{\phi}_2^2 - \frac{1}{2}\dot{\phi}_2^2\phi_2^2) = 0,\end{aligned} \tag{1.13a}$$

$$l_1\ddot{\phi}_1 + g\phi_1 + \ddot{z}\phi_1 = 0, \tag{1.13b}$$

$$l_2\ddot{\phi}_2 + g\phi_2 + \ddot{z}\phi_2 = 0. \tag{1.13c}$$

It is noted that only small deflections from equilibrium are correctly approximated. Still one can study possible strong responses of the nonlinear system to periodic perturbations. At the moment the deflections grow large only qualitative information is obtained from this approach. The solutions for the uncoupled equations are given by

$$z(t) = a_0\sin(\omega_0 t) + b_0\cos(\omega_0 t), \tag{1.14a}$$

$$\phi_1(t) = a_1\sin(\omega_1 t) + b_1\cos(\omega_1 t), \tag{1.14b}$$

$$\phi_2(t) = a_2\sin(\omega_2 t) + b_2\cos(\omega_2 t), \tag{1.14c}$$

$$\omega_0 = \sqrt{\frac{k}{M + m_1 + m_2}}, \quad \omega_1 = \sqrt{\frac{g}{l_1}}, \quad \omega_2 = \sqrt{\frac{g}{l_2}}. \tag{1.14d}$$

1.4.2 Series Solutions based on the Mathieu equation

In this section we explore the possible application of a Galerkin type of approximation of the solution of Eq.(1.13). This approach is widely used and, in the way it applies to this problem, it is also known as the "spectral method", see [2].

Since all equations of motion are invariant under time translations, we have the freedom of taking $a_0 = 0$, because later $z(t)$ can be shifted in time, and all solutions of ϕ_1 and ϕ_2 with it. We insert the harmonic solution $z(t) = b_0\cos(\omega_0 t)$ in Eqs.(1.13bc). Introduction of a new independent variable $x \equiv (\omega_0 t)/2$ transforms both equations into the Mathieu equation:

$$\frac{d^2y}{dx^2} + [a - 2k^2\cos(2x)]y = 0, \quad k^2 = q. \tag{1.15}$$

It has periodic solutions for infinitely many a, depending on the value of q. Four series of these 'eigenvalues' a do exist, and correspond to four possible combinations $k, l \in \{0, 1\}$ in the general series of solutions (Gradshteyn and Ryzhik [14]):

$$f_{kl}(x) = (\cos(x))^k \sum_{n=0}^{\infty} f_{kln}(\sin(x))^{2n+l}. \tag{1.16}$$

The derivative $(df_{kl})/(dx)(x)$ can be expressed as $g_{(k+1)(l+1)}(x)$ with a series expansion as given by Eq.(1.16) and with indices taking values modulo 2. In a similar way we handle $(d^2 f_{kl})/(dx^2)(x) = h_{kl}(x)$. For a product $p_{k_1 l_1}(x) q_{k_2 l_2}(x)$ we can derive an expression of the form $r_{(k_1+k_2)(l_1+l_2)}(x)$ with again indices that are taken modulo 2.

Let us ignore the perturbation of the heave motion by the pendulums and replace the solution $z = b_0 \cos(2x)$ by

$$z = \sum_{n=0}^{\infty} z_n (\sin(x))^{2n}. \tag{1.17}$$

Then we can express the solutions of the pitch- and roll equations as

$$\phi_i(x) = (\cos(x))^{k_i} \sum_{n=0}^{\infty} (\phi_i)_n (\sin(x))^{2n+l_i}. \tag{1.18}$$

For z it is important to take $k = l = 0$ to have the same 'overall' k and l for all terms in Eq.(1.13a) . For ϕ_1 and ϕ_2, k and l are not fixed by Eqs.(1.13bc), mainly because their first derivatives appear quadratically in Eqs.(1.13). Since products of series do couple all coefficients, it is not expected that the nonlinear recursion relations give analytical results. However, taking only the first 5 terms in the series representations, for explicit values of the constants one can numerically solve the equations for the coefficients. A stable solution with strong pitch and roll indicates the possibility of parametric roll.

1.4.3 Effect of head waves

If we include forcing from waves coming in with an angular velocity ω_0 and if we also assume that it only acts upon heave being heavily damped, then the system (1.14a)-(1.12bc) covers separately the 1-DOF model for roll (Section 1.2) as well as for pitch. If wave forcing is added to DSPM (12), then we arrive at a type of model with periodic forcing. A new element is brought in if the pitch-pendulum is considered to be directly forced by the head waves. It is known that heavy roll occurs at wave length of about the length of the ship. This means that the pitch motion will have a component with the wave frequency and an additional energy flow is expected from the pitch motion to heave and roll. Resonant forcing of the pitch motion would even enlarge this energy flow.

1.5 Stochastic aspects

Up to now we have only considered the response of a ship that encounters a single frequency wave. In reality, the sea state is a complex mixture of waves with many different frequencies, and in this section we describe possible approaches to this more difficult problem.

1.5.1 Stochastic description of ocean waves

Realistic sea states are conveniently described by their spectral properties, see Podgorski et al. [20]. Let $\zeta(t)$ denote the sea surface elevation at time t. It is assumed that this is a weakly stationary ergodic random process, which is usually satisfied for deep water waves. More specifically, $\zeta(t)$ can usually be assumed to be a Gaussian process (whose variance characterizes the sea severity) [19]. Its autocorrelation function is defined as expectation

$$R(\tau) = \lim_{T\to\infty} \frac{1}{2T} \int_{-T}^{T} (\zeta(t) - \mu)(\zeta(t+\tau) - \mu)\, \mathrm{d}t, \tag{1.19}$$

where μ is the mean surface elevation, usually chosen to be zero. By the Wiener-Khintchine theorem, the power spectral density $S(\omega)$ is given as the Fourier transform of $R(\tau)$,

$$S(\omega) = \frac{1}{\pi} \int_{-\infty}^{\infty} R(\tau) e^{-i\omega\tau}\, \mathrm{d}\tau, \tag{1.20}$$

and represents the average wave energy (density) for a given frequency component.

The sea state is generated by the complex interaction of the local wind field with the sea surface, and therefore this stochastic description is often adequate. Moreover, the spectral density $S(\omega)$ can be calculated from first principles (see e.g., [18]). In practice, however, it is more conveniently described by phenomenological models.

The Pierson-Moskowitz spectrum describes a *fully-developed* sea, i.e., a sea state that is in equilibrium with the local wind field:

$$S(\omega) = \frac{\alpha g^2}{\omega^5} \exp\left[-0.74 \left(\frac{\omega_0}{\omega}\right)\right], \tag{1.21}$$

where $\alpha = 8.1 \times 10^{-3}$, $g = 9.81\mathrm{m/s}^2$ is the usual gravitational acceleration, and $\omega_0 \approx g/(1.026 \cdot U_{10})$ depends on the wind speed U_{10} at 10 meter height. An example for different wind speeds is shown in Figure 1.7a.

The JONSWAP (Joint North Sea Wave Project) spectrum in Figure 1.7b takes into account that most sea states are rarely fully developed. It features the additional parameter F, the so-called *fetch*, which represents the distance over which the wind blows with

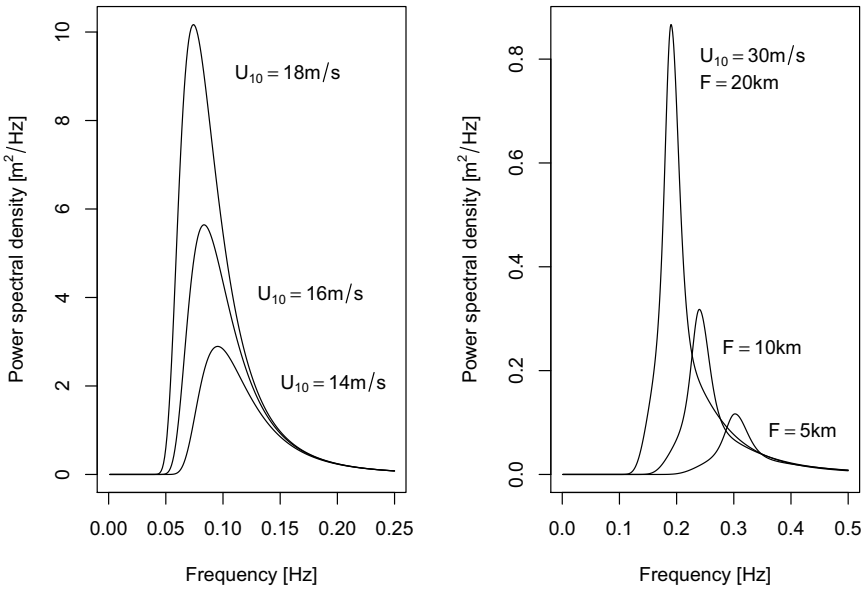

Figure 1.7: Widely used wave spectra for stochastic simulation. (a) Pierson-Moskowitz spectrum for a fully developed sea. (b) JONSWAP spectrum for the North Sea for different values of the fetch (see text). Note that the JONSWAP spectrum does not represent a fully developed sea!
different

constant velocity U_{10}. Explicitly, it is given by

$$S(\omega) = \frac{\alpha g^2}{\omega^5} \exp\left[-\frac{5}{4}\left(\frac{\omega_p}{\omega}\right)^4\right] \gamma^r, \quad r = \exp\left[-\frac{(\omega-\omega_p)^2}{2\sigma^2\omega_p^2}\right], \tag{1.22}$$

where now $\alpha = 0.076(U_{10}^2/(F \cdot g))^{0.22}$, $\omega_p = 22(g^2/(U_{10} \cdot F))^{1/3}$, $\gamma = 3.3$, and $\sigma = 0.07$ for $\omega \leq \omega_p$, and $\sigma = 0.09$ otherwise.

Sometimes an additional component is visible in real spectra, the so-called *swell*. This is caused by a distant wave field that has travelled into the area and is superimposed on the locally generated field.

1.5.2 Simulations

Knowledge of $S(\omega)$ allows the efficient simulation of the underlying process, by approximating it by a finite mixture of frequencies. Assuming that the process $\zeta(t)$ is bandlim-

ited[2], i.e., $S(\omega)$ is zero outside an interval $[-\Delta, \Delta]$, let us divide the interval $[0, \Delta]$ into N subintervals of length Δ/N. Then we can write

$$\tilde{x}(t) = \sum_{k=1}^{N} A_k \cos(\omega_k t + \epsilon_k), \tag{1.23}$$

and the process $\tilde{x}(t)$ exhibits (approximately) the same stochastic properties as $\zeta(t)$. Here the phases ϵ_k are chosen uniformly from the interval $[-\pi, \pi]$, and the amplitudes A_k are given by $A_k = 2\left(S(\omega_k)\Delta_k\right)^{1/2}$. This method goes back to the seminal work of Rice [22], and has been widely used in applications. It is also the basis for the recently developed *surrogate data* methods in nonlinear time series analysis. However, mathematically it is preferable to use

$$x(t) = \sum_{k=1}^{N} R_k \cos(\omega_k t + \epsilon_k), \tag{1.24}$$

where R_k has a Rayleigh distribution with parameter $2S(\omega_k)\Delta_k$ [29].

Instead of using a regular division of the power spectral density, one can also sample frequency components randomly, according to the probability density

$$p(\omega) = \frac{S(\omega)}{\sigma^2}, \tag{1.25}$$

where $\sigma^2 = \int_0^\infty S(\omega)\, \mathrm{d}\omega$ is the variance of $\zeta(t)$ [16].

A drawback of both these methods is (i) that the spectrum of the simulated elevations is discrete, and (ii) that the process $\zeta(t)$ is only approximated well for N sufficiently large. To overcome this limitation, one can consider a *disordered periodic process*,

$$y(t) = \sum_{k=1}^{N} B_k \cos(\omega_k t + \nu_k), \tag{1.26}$$

where the ν_k are independent white-noise processes. This leads to a continuous spectrum and even allows the derivation of analytical results in a few special cases, applying the theory of stochastic differential equations [1, 16, 21]. However, there is no simple relation between the spectra of $\zeta(t)$ and $y(t)$, and the former therefore needs to be fitted nonlinearly to $S(\omega)$.

Finally, for simulation purposes the most efficient representation is in terms of a time-discrete ARMA(P,Q) process,

$$z_t = \sum_{k=1}^{P} a_k z_{t-k} + \sum_{l=1}^{Q} b_l \epsilon_{t-l} + \epsilon_t, \tag{1.27}$$

[2]In practice, the cut-off frequency Δ is usually chosen to be the Nyquist-frequency with which the data have been sampled.

where the ϵ_t are uncorrelated Gaussian white-noise errors. As before, the coefficients need to be found by nonlinearly fitting the spectrum of z_t to $S(\omega)$. These processes have been popularized by Spanos and Mignolet [27].

Multivariate generalizations of these techniques also exist. In particular, if one is interested in a specific sea state, from which time series recordings are available, the nonparametric simulation technique of DelBalzo et al.[4], going back to earlier work of Scheffner and Borgman [25], can be employed [4]. Thereby, the variables of interest (sea elevation, wave periods, wave directions, etc.) are transformed to (correlated) Gaussian variables. Realizations of these with the desired correlation structure can then be easily obtained from the eigendecomposition of the covariance matrix, and transformed back into time series.

1.5.3 Nonstationary sea states

In the above, we have still assumed that the sea state is stationary. This assumption is often warranted for timescales of up to a few hours to days, but in general it is clear that the properties of the sea change over the course of time.

The standard methods to deal with this issue are so-called sea-state *prediction graphs* (e.g., see Table 2.2 in [7]). These are basically discretized probability distributions of wave spectra that state the probability to find a given wave spectrum in a random observation interval. From these, a nonstationary time series of surface elevations $\zeta(t)$ can be achieved as a hidden Markov process, where a continuous-time Markov chain allows the process to switch from one wave spectrum to another regime.

1.5.4 Connection with ship dynamics

How do the above considerations connect with the dynamical evolution of the state of a ship? We have already seen in Eq.(6) that the equations of motions are uncoupled to first order in the parameter η with respect to roll motion. Excitation of roll motion is facilitated through a restoring moment $\gamma(\varphi, t)$, that is given by the so-called *righting lever curve* for the ship under consideration. In calm water, this moment is time-independent, but in general the righting-lever curves capture the effect of dynamical changes in stability and depend on wave properties and the ship's speed. The slopes of these curves in the upright position correspond to the variation in metacentric height GM that the ship experiences, and the restoring moment can be modelled by

$$\gamma(\varphi, t) = (1 + \delta \cos \omega t)\varphi - \alpha\varphi^3, \tag{1.28}$$

where 2δ corresponds to this variation, and ω is the wave encounter frequency [16]. Note that the latter is related to the wave frequency ω_0 by a Doppler shift, $\omega = \omega_0 - \omega_0^2 U/g \cdot \cos\mu$, where μ is the angle between wave propagation and the ship's forward direction, and U is the ship's speed. The additional parameter α captures the nonlinearity of the restoring lever curves and can be fitted from available design data.

The effect that a sea state will have upon the motion of a ship is usually expressed in terms of the so-called *response amplitude operator*, which is the transfer function for the linear ship model and readily available for most ship designs. An external forcing by a frequency component

$$A_k \cos(\omega_k t + \epsilon_k) \tag{1.29}$$

will result in a steady-state response

$$A_k |H(\omega_k)| \cos(\omega_k t + \delta(\omega_k) + \epsilon_k), \tag{1.30}$$

where $|H(\omega_k)|$ is the frequency-dependent response per unit wave amplitude and $\delta(\omega_k)$ is a phase angle [7].

The beauty of linear equations of motion is that the response amplitude operators corresponding to distinct frequency components can be simply superposed.

1.5.5 Risk quantification

As the dynamical system of the ship is nonlinear and nonautonomous, it is almost impossible[3] to find analytical results for its stability under random sea states, even if the stochastic properties of the latter are known.

In practise one is interested in a quantification of the *risk* of occurence of parametric roll resonance. Assuming that the *loss* is total when the roll angle rises above a certain threshold (e.g., 20 degrees, as then containers are likely to fall off from a container ship), simplifies the problem enormously. Assuming that such an event is unlikely, it can be mathematically modelled as a homogeneous Poisson process with intensity $\lambda > 0$, whereby λ represents the expected number of events per unit time. Let N be the number of such events during a fixed time of operation T of the ship, then

$$\mathrm{pr}(\text{loss}) = \mathrm{pr}(N \geq 1) = 1 - e^{-\lambda T} \tag{1.31}$$

is the desired risk of loss.

We can estimate λ from numerical simulations, resetting the simulation to randomly chosen initial conditions whenever the roll angle exceeds the threshold, and counting

[3]The work of Farrell et al. on generalized stability theory [8] could offer a possible way to deal with these problems.

the occurences of these events. However, it is more advantageous to consider the mean waiting time τ before such an event occurs. The interarrival times in the Poission process are exponentally distributed, and the relation between τ and λ is simply $\tau = 1/\lambda$.

Since expectation is a linear operation, it is clear that one only needs to estimate λ for each stationary sea state of interest, characterized by a single wave spectrum, and can use the above-mentioned prediction graphs (or a hidden Markov model, for a more accurate estimate) to combine risks for different sea states into a global *operational risk*.

Alternatively, one could use extreme value statistics [3], e.g., by fitting the maxima of roll angles observed in a simulation to an extreme value distribution. This would be particularly useful to quantify the operational risk in conditions where resonance might be expected, but occurs too seldomly to calculate mean waiting times.

1.5.6 Numerical results

Stochastic waves generated by (24) act upon the vessel. Therefore, *effective* transfer functions have to be used with the appropriate parameters such as damping constants and added masses. The values of these constants are weighted averages over 500 frequency components of a random Pierson-Moskowitz spectrum, weighted according to spectral power. Figure 1.8 shows an example for wind speed $U_{10} = 21$ m/s. The wave time series has been generated by the method of Rice (Section 1.5.2) from the random spectrum shown on the right of it. For comparison, also the corresponding analytical Pierson-Moskowitz spectrum is depicted. Such a wind speed (Beaufort scale 8.3) results in a rough sea with a significant wave height of 5.9 meters. Although the ship heaves with a comparable amplitude, there is no parametric rolling. In contrast to that, increasing the wind speed to $U_{10} = 22$ m/s leads to the situation in Figure 1.9. For such wind conditions (Beaufort scale 8.6) the significant wave height amounts to 7.8 meters and stochastic resonance occurs.

Finally, Figure 1.9 shows a risk function for the occurrence of parametric roll under Pierson-Moskowitz spectra. The data is based on 100 simulations that stopped either when the roll angle exceeded 20 degrees, or after 10 hours simulated time, if no resonance could be observed during that time. Each simulation is based on a different randomly generated spectrum, starting from small initial conditions (0.01 meter heave and 1.0 degree roll) and the mean waiting time was recorded. The finite simulation time introduces a bias, since some waiting times are *censored* meaning that only a lower bound is known. For simplicity, this effect was corrected by subtracting the minimal possible rate (one event per 10 hours) from the corresponding mean rate $\bar{\lambda} = 1/\bar{\tau}$. The minimal observed

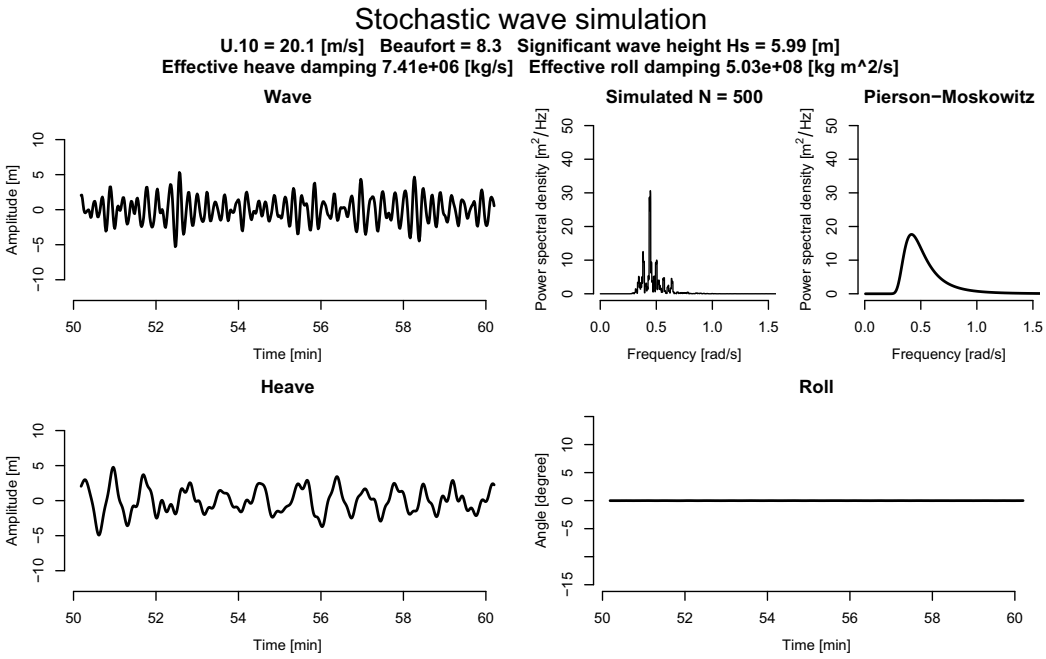

Figure 1.8: Example of stochastic simulation. Top left: Time series of wave heights generated by the method of Rice [22]. Top right: Spectrum of generated wave heights and the corresponding analytical Pierson-Moskowitz spectrum. Bottom left: Heave motion of the ship in the pendulum-spring model under this wave forcing. Bottom right: Roll angle. Results shown are for a wind speed of 8.3 Beaufort. Note that roll resonance does not occur.

fraction of events (three events, for $U_{10} = 18$ m/s) was added to the values obtained from Eq.(1.31) and the result is the approximate operational risk shown in Figure 1.10.

Note that this example just illustrates the methodology. In particular, the simple pendulum model is difficult to use with stochastic waves, since the equivalent pendulum length L, and the damping and stiffness constants depend explicitly on the wave frequency. Using effective values as here is only a rough approximation and serves to illustrate the procedure; in reality, one would need to use a different dynamical model that accounts for these frequency-dependent effects.

1.6 Recommendations for Future Investigations

In the study of the rolling motion of a vessel as it is forced by waves we discern two mayor directions:

- Analysis of the nonlinear dynamical equations stressing the interaction of different

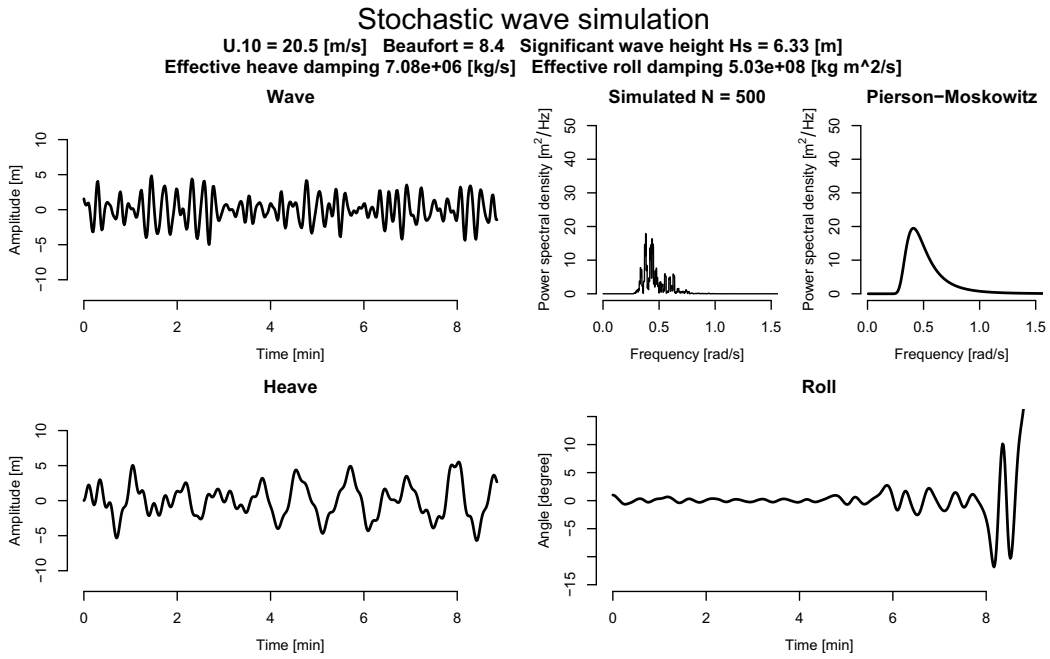

Figure 1.9: Example of a stochastic simulation as in Figure 1.7. Results shown are for a slightly larger wind speed of 8.4 Beaufort. Now roll resonance does occur.

modes (heave, pitch, and roll) and the possibility of (parametric) resonance.

- The stochastic description of ocean waves and their effect upon the metacentric height change of the vessel.

Of course also other aspects of the problem play a role such as the computation of dynamical parameters from the design and loading of a vessel. In our search for causes of extreme roll in heavy seas these studies play an ancillary role. For each of the two directions indicated above we bring up ideas for further research which possibly may lead to a better understanding of the problem of extreme roll resulting in solutions remedying this unwanted phenomenon.

From the point of view of modeling ship motion by nonlinear differential equations 3-DOF models fully cover the motion of a ship if we consider it as a point mass and ignore displacement in the horizontal plane. In Section 1.4 we discussed one such a model being an alternative to a model analyzed in [30]. Of course the number of degrees of freedom can easily be extended, see Korvin- Kroukovsky [15]. However, we have the idea that for a 3-DOF system not yet all possible causes of extreme roll have been identified. In particular the fact that this phenomenon occurs in combination with waves having a wavelength in the order of the length of the vessel suggests that forcing is not only through the heave

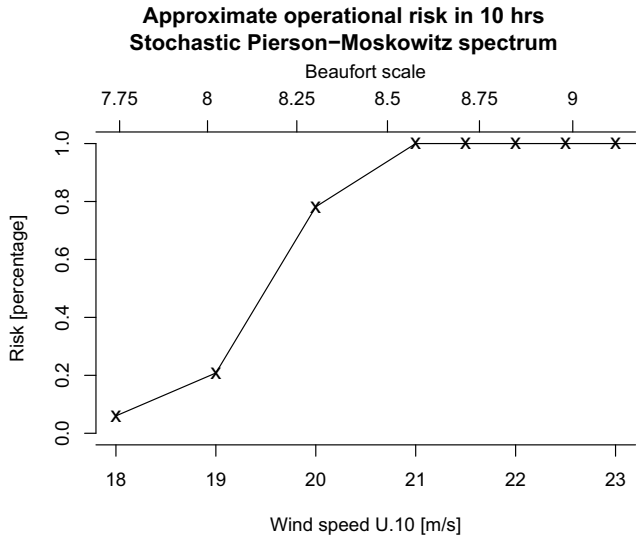

Figure 1.10: Risk of parametric roll (angle larger than 20 degrees) for waves having a Pierson-Moskowitz spectrum at different wind speeds.

mode of the system but also through pitch. If this component of the forcing is present, then in a short time a large amount of energy can be transferred from the waves to the ship motion, as we already pointed out in Section 1.4. If in addition the forcing frequency is close to the natural pitch frequency, the roll amplitude may increase even more. It is worth to have this analyzed. Furthermore in Section 1.4 it is pointed out that the solution of systems with small DOF's can be approximated by series expansions based on series solutions of the Mathieu equation.

In Section 1.5 it is suggested that the most efficient representation of stochastic waves is that of a linear ARMA-system see Eq.(1.27). This approach can also be used in the stochastic description of roll forced by waves as presented by Dunwoody [5]. He formulates the Langevin equations for roll amplitude and phase, see formula's (5-6) of [5]. Instead of solving the equation for the corresponding Fokker-Planck equation one can formulate the exit problem for the amplitude exceeding some large value. It yields the expected value for the time needed to arrive at this value, see [11]. This exit time quantifies the risk of extreme roll better than the mean amplitude.

Bibliography

[1] Arnold, L., Chueshov, I., and Ochs, G. (2004). Stability and capsizing of ships in random sea — a survey. *Nonlinear Dynamics*, 36:135–179.

[2] Boyd, J. (2001). *Chebyshev and Fourier Spectral Methods*. Dover Publications.

[3] Coles, S. (2001). *An Introduction to Statistical Modelling of Extreme Values*. Springer-Verlag.

[4] DelBalzo, D., Schultz, J., and Earle, M. (2003). Stochastic time-series simulation of wave parameters using ship observations. *Ocean Engineering*, 30:1417–1432.

[5] Dunwoody, A. (1989). Roll of a ship in astern seas response to gm fluctuations. *Journal of Ship Research*, 33(4):84–290.

[6] Eissa, M., El-Sera, S., El-Sheikh, M., and Sayeda, M. (2003). Stability and primary simultaneous resonance of harmonically excited non-linear spring pendulum system. *Appl. Math and Computation*, 145:421–442.

[7] Faltinsen, O. M. (1993). *Sea Loads on Ships and Offshore Structures*. Cambridge University Press.

[8] Farrell, B. and Ioannou, P. (1996). Generalized stability theory. Part II: Nonautonomous operators. *Journal of the Atmospheric Sciences*, 53:2041–2053.

[9] France, W., Levadou, M., Treakle, T., Paulling, J., Michel, R., and Moore, C. (2003). An investigation of head-sea parametric rolling and its influence on container lashing systems. *Marine Technology and SNAME News*, 40(1):1–19.

[10] Francescutto, A. and Bulian, G. (2004). Nonlinear and stochastic aspects of parametric rolling modelling. *Marine Technology*, 41(2):74–81.

[11] Grasman, J. and van Herwaarden, O. (1999). *Asymptotic Methods for the Fokker-Planck Equation and the Exit Problem in Applications*. Springer-Verlag, Berlin Heidelberg.

[12] Hochstadt, H. (1986). *The Functions of Mathematical Physics*. Dover Publications.

[13] Holden, C., Galeazzi, R., Rodrìguez, C., Perez, T., Fossen, T., Blanke, M., and de Almeida Santos Neves, M. (2007). Nonlinear container ship model for the study of parametric roll resonance. *Modeling, Identification and Control*, 28(4):87–103.

[14] Jeffrey, A. and Zwillinger, D. (2007). *Gradshteyn and Ryzhiks Table of Integrals, Series and Products*. Academic Press.

[15] Korvin-Kroukovsky, B. (1961). *Theory of Seakeeping*. Soc. Naval Architects and Marine Engineers, New York.

[16] Kreuzer, E. and Sichermann, W. (2006). The effect of sea irregularities on ship rolling. *Computing in Science & Engineering*, 8(3):26–34.

[17] Levadou, M. and van't Veer, R. (2006). Parametric roll and ship design. In *Proceedings of the 9th International Conference on Stability of Ships and Ocean Vehicles*.

[18] Massel, S. (1996). *Ocean Surface Waves: Their Physics and Prediction*. World Scientific Publishing.

[19] Ochi, M. (2005). *Ocean Waves: The Stochastic Approach*. Cambridge University Press.

[20] Podgorski, K., Rychlik, I., and Machado, U. (2000). Exact distributions for apparent waves in irregular seas. *Ocean Engineering*, 27:9791016.

[21] Poulin, F. and Flierl, G. (2008). The stochastic Mathieu's equation. *Proceedings of the Royal Society A*, 464:1885–1904.

[22] Rice, S. (1944). Mathematical analysis of random noise. *Bell System Technical Journal*, 23:282–332.

[23] Santos-Neves, M., Pérez, N., and Lorca, O. (2003). Analysis of roll motion and stability of a fishing vessel in head seas. *Ocean Engineering*, 30:921–935.

[24] Santos-Neves, M. and Rodríguez, C. (2007). Influence of non-linearities on the limits of stability of ships rolling in head seas. *Ocean Engineering*, 34:1618–1630.

[25] Scheffner, N. and Borgman, L. (1992). Stochastic time-series representation of wave data. *J. Waterway Port Coast. Ocean Eng.*, 118(4):337–351.

[26] Shin, Y., Belenkey, V., Pauling, J., Weems, K., and Lin, W. (2004). Criteria for parametric roll of large containerships in longitudinal seas. *Transactions – Society of Naval Architects and Marine Engineers*, 112:14–47.

[27] Spanos, P. and Mignolet, M. (1986). Z-transform modelling of P-M wave spectrum. *Journal of Engineering Mechanics*, 112:745–759.

[28] Spyrou, K. (2000). Designing against parametric instability in following seas. *Ocean Engineering*, 27:625–653.

[29] Sun, T. and Chaika, M. (1997). On simulation of a Gaussian stationary process. *Journal of Time Series Analysis*, 18:79–93.

[30] Tondl, A., Ruijgrok, T., Verhulst, F., and Nabergoj, R. (2000). *Autoparametric Resonance in Mechanical Systems*. Cambridge University Press, Cambridge.